Very large-scale motion in the outer layer

K. C. Kim* and R. J. Adrian

Department of Theoretical and Applied Mechanics, University of Illinois, Urbana, IL 61801

Very large-scale motions in the form of long regions of streamwise velocity fluctuation are observed in the outer layer of fully developed turbulent pipe flow over a range of Reynolds numbers. The pre-multiplied, one-dimensional spectrum of the streamwise velocity measured by hot-film anemometry has a bi-modal distribution whose components are associated with large-scale motion and a range of smaller scales corresponding to the main turbulent motion. The characteristic wavelength of the large-scale mode increases through the logarithmic layer, and reaches a maximum value that is approximately 12-14 times the pipe radius, one order of magnitude longer than the largest reported integral length scale, and more the 4-5 times longer than the length of a turbulent bulge. The wavelength decreases to approximately two pipe radii at the pipe centerline. It is conjectured that the very large-scale motions result from the coherent alignment of large-scale motions in the form of turbulent bulges or packets of hairpin vortices.

[PACS number 47.27.Nz]

I. INTRODUCTION

The existence of energetically significant large-scale structures in turbulent wall flow was first recognized by Townsend[1], who observed that the long tail on the temporal correlation of the streamwise velocity component measured by Grant [2] implied correspondingly long structures in the streamwise direction. The long correlation tails occur not only in the buffer layer, where the visualizations of Kline, *et al.*[3] revealed low speed streaks, but also throughout the logarithmic layer and into portions of the wake region. Subsequent investigations[4-6] indicate that one type of large-scale motion in the boundary layer occurs in the form of turbulent bulges having mean streamwise extent of approximately 2-3δ and spanwise extent of approximately 1-1.5δ where δ is the boundary layer thickness. These bulges, which are generally referred to as *large-scale motions*, or LSM's, are now widely interpreted to be the motions responsible for the long correlation tails in Grant's[2] experiments. (See for example the reviews of Cantwell[7] and Robinson[8]). It has also been shown that the turbulent bulges have steeply inclined leading fronts and more gradually sloped backs, and that the downstream back of a bulge is separated from the front of the adjacent upstream bulge by a sharp crevice in the potential flow[9, 10].

*Permanent address: School of Mechanical Engineering, Pusan National University, Pusan 609-735, Korea

Particle image velocimetry experiments in the turbulent boundary layer reveal long, growing zones of relatively uniform low streamwise momentum in the outer region, especially in the logarithmic layer[11]. These structures may be related to turbulent bulges, but two features suggest that the relationship is not a simple correspondence. First, the zones of uniform momentum have much more streamwise coherence in the lower half of the boundary layer than in the upper half. Second, two zones of uniform momentum often co-exist, one above the other in the lower half of the boundary layer, showing that they do not coincide one-for-one with turbulent bulges. Zhou, *et al.*[12-14] conclude that the uniform momentum zones are formed by the streamwise alignment of hairpin or cane vortices in packets that grow and generate new hairpins as they propagate downstream. The induced flow associated with each vortex has low streamwise momentum, and the summation of the induced flow fields from all of the aligned hairpins creates a long streak of low momentum fluid. The PIV observations in these experiments were limited to 1.2δ, and the hairpin packets often exceeded this length, leaving their maximum extent undetermined. More recent work using PIV measurements spanning 3δ indicates that the hairpin packets may be associated with the formation of bulges, but that several packets, at various stages of growth can exist within one bulge[15].

A recent model of wall turbulence[16] recognizes the need to extend earlier hairpin vortex models[17, 18] by incorporating one set of large-scale eddies. Its length scale was set equal to δ, corresponding to the length of a turbulent bulge. The large-scale motion is necessary to model correctly all components of the Reynolds stress tensor and to improve the model's prediction of the wake structure. Much of the justification for adding the large-scale component to the model and for scaling it on δ comes from inspection of turbulence spectra which indicate a low-wavenumber component that corresponds, presumably, to the long tail on the correlation function.

While most of the available studies of large-scale motions have concentrated on the turbulent boundary layer, there is evidence that large-scale motions of a broadly similar nature also exist in turbulent pipe flow. Measurements of temporal correlation in pipe flow show a long tail on the correlation function that is similar to that observed in the boundary layer[18-20]. In pipe flow the longitudinal integral length scale of the streamwise velocity, L_{11}, measured from two-point correlations or estimated from temporal correlations using Taylor's hypothesis and the local mean velocity, is approximately 0.5-1R, where R is the pipe radius. In comparison, the integral length scale of the boundary layer is approximately 0.5δ. Thus, there is an approximate correspondence between the boundary layer thickness and the pipe radius that can be used to compare the sizes of large-scale structures found in these flows. The large-scale motions in pipe flow are undoubtedly influenced by the constraints imposed by the geometry of the pipe (as opposed to the unconfined geometry of a boundary layer). But, the close similarity of mean properties measured in the lower

half of the pipe radius and the boundary layer thickness suggests that these differences are not great. Since the integral length scales are similar, it would not be surprising to observe large-scale motions as large as 2 -4R in pipe flow, in analogy to the bulges that occur in the boundary layer.

In contrast to what might be expected from the foregoing arguments, the results of the present study demonstrate the existence of a new type of large-scale motion that is much longer than the LSM's that correspond to bulges or hairpin packets. These very large-scale motions, or VLSM's, are prominent within the logarithmic layer of turbulent pipe flow. Evidence for the VLSM's is based on extensive measurements of the turbulent power spectrum of the streamwise velocity fluctuation in a fully developed turbulent pipe flow at Reynolds numbers ranging from 33,800 to 115,400. The turbulent spectra are interpreted to consist of two modes, one of them representing large-scale motions. The wavelength associated with the middle of the large-scale range varies as a function of Reynolds number and radial position of the pipes.

II. EXPERIMENTAL APPARATUS AND METHODS

The pipe flow facility was a 17m long Plexiglas pipe having diameter 2R= 127mm. Air from a blower passed through a settling chamber, a honeycomb, and a grid before it entered the pipe. The grid flattened the initial velocity profile and reduced the inlet length required for the flow to become fully developed. All measurements were made with a single hot-film probe located two diameters upstream of the open exit from the pipe, corresponding to 134 diameters of development length. The characteristics of the flow in this apparatus, including measurements of the complete time-delayed correlation tensor, have been documented thoroughly by Lekakis[20]. The pipe apparatus produces flow whose mean properties are consistent with the results of numerous other pipe flow experiments, to within normal standards of experimental comparison. Therefore, we consider the present flow to be representative of typical pipe flows.

The parameters of the experiments are given in Table 1, where U_c is the centerline velocity and u_τ is the friction velocity determined directly from the pressure drop measured by wall pressure taps located at 37 and 100 diameters downstream of the pipe inlet in a region of fully developed flow. Two devices measured the pressure difference: an inclined manometer for high velocities and an electronic pressure transducer with resolution ±0.0001 mm H_20 for low velocities.

The streamwise velocity was measured by a 25.4μm diameter platinum hot-film sensor (TSI 1210-20) operated by a TSI model 1750 constant temperature anemometer at 1.7 overheat ratio. The frequency response of the sensor, determined by a square wave test, was greater than 35 kHz. The signal from the anemometer was direct-coupled to preserve the low frequency content, and low-pass filtered for anti-aliasing prior to sampling with a 12-bit A-D converter (National Instrument Lab PC+). A LabView virtual instrument program was used to acquire data and

calculate the power spectral density function $\Phi_{11}(\omega)$ using a FFT algorithm and a Hanning window, where $\omega = 2\pi f$ is the radian frequency. Ensembles of 100 records, each record containing 16,384 samples taken at the frequency listed in Table 1, were used to estimate the power spectrum at each of 35 radial locations.

To transform the spectral argument from frequency, ω, to streamwise wave number, $k_1(y)$, Taylor's hypothesis of frozen turbulence was used, i.e., $k_1=2\pi f/U(y)$, wherein the local convection velocity is assumed to be equal to the local mean velocity U(y). It is understood that Taylor's hypothesis is not accurate for the very large-scales considered here; however, the time-delayed correlation should decay faster than the two-point spatial correlation due to evolution of the turbulent eddy structures as they pass over the probe, so wavenumber spectra derived from frequency spectra must indicate less low wavenumber energy than true wavenumber spectra. Hence, wavelengths determined from the frequency spectra by Taylor's hypothesis are underestimated; but this underestimate only strengthens the principal conclusion of this paper, which is that the very large-scale motions exist that are substantially longer than expected.

The possible influence of an organ pipe effect has been examined carefully. A sharp resonant peak did appear at 29.5Hz, which is the estimated organ pipe frequency in all of the measurements. However, the relative power was small (0.9 % at the lowest Reynolds number and 0.013 % at the highest Reynolds number). Moreover, changing the organ pipe frequency relative to the turbulence spectrum had no discernible effect on the broad-band spectrum.

III. Results and Discussion

Fig. 1 shows a typical frequency spectrum of the streamwise velocity after conversion into a normalized wave-number spectrum, $\Phi_{11}(k_1R)/u_\tau^2$ using Taylor's hypothesis. The location of the measurement, y/R = 0.084 (corresponding to y^+ =132) lies above the buffer layer and in the lower portion of the logarithmic layer. The spectrum appears to possess a k^{-1} power law, as observed by Perry and co-workers[17, 18], and it may possess a short region of $k^{-5/3}$ power law. It is generally similar to spectra obtained in other pipe flows, and in channel flow and boundary layers.

The structure of the spectrum in Figure 1(a) is easier to interpret when plotted as the wavenumber times the spectrum, Figure 1(b). The usual reason for pre-multiplying the spectrum by the wavenumber is to create a logarithmic plot in which equal areas under the curve correspond to equal energies. The other reason is to reveal the region of k_1^{-1} power law behavior. When viewed in this way the spectra of wall turbulence also exhibit an interesting structure that allows for a different interpretation. In particular, there is a peak at low wave number (labeled A) followed by

a region of relatively constant wave number (which Perry and co-workers attribute to the k^{-1} power law region of the matching layer), and then a rapid decrease that begins at the low frequency end of the inertial subrange. We interpret the shape of the complete spectrum to be a summation of two modes: a low wave number mode labeled A and the high wave number mode labeled B. This shape is quite typical of the measurements found in Perry and Abell[21], Bullock, *et al.*[22] and Lekakis[20] for pipe flow and Perry, Henbest and Chong[18] for boundary layers. The separation of the spectrum into two separate modes cannot, of course, be carried out uniquely, but for the purpose of illustrating the bimodal interpretation, dashed lines have been sketched in Figure 1(b) to approximate two modes whose sum would correspond to the observed total curve.

It can be shown that the two modes scale on inner and outer variables, respectively. The plot in Fig. 2, which uses dimensionless coordinates based on the viscous length scale, clearly shows that the high wavenumber component scales with inner variables, independent of Reynolds number. The corresponding plot in terms of outer variables, Fig. 3 shows that the low wavenumber mode scales much more closely with outer variables than inner variables. In, particular, the locations of the maxima of the low wavenumber component are insensitive to the Reynolds number. These observations support the interpretation of the spectrum as consisting of two modes: a low wavenumber mode that scales with outer variables, and a high wavenumber mode that scales with inner variables. This interpretation is useful because it gives physical significance to the low wavenumber maxima that occur in the pre-multiplied spectra. However, the bimodal interpretation is not essential, because the wavenumber at which a low wavenumber maximum occurs can be determined independently of the existence of a bimodal distribution.

The mode shapes vary with radial location and Reynolds number, as illustrated by the spectra in Figure 4 for Re=115,400. At some radial locations it is difficult to distinguish a high wavenumber mode, but it is always possible to identify the low wavenumber mode by the maximum in the pre-multiplied spectrum (indicated by the arrows). We use the location of the maximum, $2\pi/\Lambda_{max}$ to indicate the scale of the very large-scale motions, Λ_{max}.

Figure 5 plots the values of the wavelength Λ_{max} versus distance from the wall for varying Reynolds numbers. Over the range of Reynolds numbers in this study there is a generally consistent trend for Λ_{max} to begin at a value less than 2 pipe radii near the wall, increase rapidly to values between 12-14 pipe radii between $0.25R<y<0.45R$, and then to decrease to approximately 2 pipe radii at the center of the pipe. Analysis of the pipe data of Perry and Abell[21], Bullock, *et al.*[22] and Perry *et al.*[18] yields results consistent with the present experiments. (The data of Perry *et al.*[18] in Fig. 5 are shown as a straight line because of the large number of data involved.) A Reynolds number effect occurs in Fig. 5 above $y/R > 0.3$. The wavelength at the lowest Reynolds number drops abruptly from its maximum value of 10R at $y/R=0.25$, but at the two higher Reynolds

numbers the corresponding drop does not occur until approximately y/R=0.4. The similarity of the two curves at the two higher Reynolds numbers suggests that the flow may approach an asymptotic state for Reynolds numbers exceeding 50,000-100,000.

The most interesting aspect of Figure 5 is the extraordinarily large extent of the very large-scale motion in the streamwise direction. The peak value of Λ_{max}, approximately 12-14R, is much larger than any value previously reported for the large scales. For comparison, the integral length scale L_{11} increases monotonically in y and reaches a maximum value of approximately 0.5-1R[19]. In contrast, Λ_{max} has a non-monotonic distribution with a peak value 12-28 times larger than the maximum value of L_{11}. For further comparison, the average turbulent bulge in a boundary layer is approximately 2-3 boundary layer thickness long, corresponding approximately to 2-3R in pipe flow. The maximum value of Λ_{max} is 4-5 times bigger. Since the term "large scale motion" or LSM now commonly refers to the bulges in boundary layers, we will refer to the longer motions identified here as "very" large-scale motions, or VLSM's. The region in which the VLSM's occur extends from roughly the top of the buffer layer to y/R~0.25-0.4. It contains the entire logarithmic region of the mean velocity profile.

The distribution in Fig. 5 suggests that the length scale measured by analysis of the spectra is associated with *two different large-scale phenomena.* One has length of order 2R and spans much of the region from the wall to the centerline. The other has length up to 14R, and it is concentrated around the logarithmic region.

Once the existence of the very large-scale components of the streamwise velocity is recognized, it is easy to see them in the time history of the signal. The data in Fig. 6., taken on the centerline of the pipe, is a typical example. For reference, the values of $2R/U \cong 0.025$ seconds and $15R/U \cong 0.2$ seconds are indicated on the figure. The 2R-long motions occur in the form of groups of more rapid oscillations. For example between $0.25 < t < 0.27$s there is a group of 6 oscillations about a low velocity excursion, and between $0.28 < t < 0.31$ there is a group of 4 oscillations about a high velocity excursion. Examples of very large-scale motions occur between $0 < t < 0.14$s, and between $0.06 < t < 0.36$s, the later corresponding to 23R. This behavior, with proper accounting for changes of the mean velocity, is observed in all of the time histories we have examined.

IV. A Physical Model

The foregoing results make a compelling case for the existence of very large-scale motions in pipe flow. While the data are not sufficient to definitively explain the underlying fluid mechanical mechanisms that create these motions, there are enough clues to at least formulate a conjecture. In

time histories such as Fig.6 the rapid fluctuations have periods less than 5ms, which corresponds to about 400 viscous length scales. This is within a factor of two of the length of the low-speed streak associated with an individual hairpin vortex[13], making it plausible to interpret the rapid oscillations as the signature of the passage of individual hairpins. The rapid oscillations occur in groups of 3-10 whose durations are of the order of 2R/U, indicating that the hairpins occur in groups that are approximately 2R long, on average. These properties closely resemble those of the hairpin packets that have been identified in earlier investigations[12-15]. (The work of Tomkins[15] indicates that mature packets of hairpins and bulges in the boundary layer appear to be parts of the same motion, so it is not, perhaps surprising that the length of a typical group in the present study is approximately equal to the mean length of a bulge.) Beyond this scale, there is, quite evidently, a mode with average wavelengths of the order of 15R/U.

A simple hypothesis that avoids asserting that the VLSM constitutes a new type of turbulent motion is to conjecture that the VLSM is a consequence of spatial coherence between bulges or between packets of hairpins. In this picture, the packets line up so that the low momentum flow in the lower part of each packet fits together with the flows in the other packets to form a much longer structure. The VLSM's are associated with the zones of uniform low momentum found in the boundary layer in each packet[11, 13,15]. These zones extend up to about one-half of the boundary layer thickness, and they are believed to be the consequence of hairpin vortices aligning in the streamwise direction to create large streams of low momentum fluid[11, 13,15]. The packets and the associated hairpin packets are sketched in Fig. 7. If there is a correlation of the motion between turbulent bulges so that they do, in fact, align, then the final result would be regions of low momentum flow that would extend over several packet lengths, consistent with the results obtained here. In this conceptual model, the VLSM's are not a new type of eddy, but merely the consequence of coherence in the pattern of hairpin packets.

IV. SUMMARY AND CONCLUSIONS

It has been shown that streamwise energetic modes in turbulent pipe flow have wavelengths that range between 2 and 12-14 pipe radii. These wavelengths are a lower bound on the actual wavelength because they have been inferred from frequency spectra, which suffer from lost correlation due to convection velocity of the components in various values. In comparison, the streamwise extent of large-scale turbulent bulge motions in boundary layers is approximately two boundary layer thicknesses. The very large-scale motions are longest in the lower half of the boundary layer. It is conjectured that the great streamwise extent of the VLSM is a consequence of large-scale motions associated with packets of hairpin eddies (Zhou, *et al.*[12-14]) aligning coherently so that the low momentum flow from the lower half of one is passed on to the next, and so on over a span of many LSM's. Thus, the hairpins align coherently in packets that are about 2R long, on

average, forming the LSM's, and then the packets align coherently to form the very large-scale motions.

An important ramification of these observations is that numerical simulations of wall turbulence may need to use longer computational domains than has been the accepted practice. Recent work by Komminaho, *et al.*[23] on very long roll cell structures in low Reynolds number DNS of plane Couette flow speaks to this same problem.

ACKNOWLEDGMENTS

This research was supported by a grant from the Office of Naval Research, N0014-97-J-0109, and one of us (HCK) and was supported by a fellowship from the Korean Science Foundation.

REFERENCES

[1]A. A. Townsend, "The turbulent boundary layer," in *Boundary Layer Research*, ed. H. Gortler, Springer-Verlag, Berlin, **1** (1958).

[2]H. L. Grant, "The large eddies of turbulent motion," J. Fluid Mech., **4**, 149 (1958).

[3]S. J. Kline, W. C. Reynolds, F. A. Schraub, and P.W. Runstadler, "The structure of turbulent boundary layers," J. Fluid Mech., **30**, 741 (1967).

[4]L.S.G. Kovasznay, V. Kibbens and R. F. Blackwelder, "Large-scale motion in the intermittent region of a turbulent boundary layer," J. Fluid Mech., **41**, 283 (1970).

[5]J. Murlis, H. M. Tsai, and P. Bradshaw, "The structure of turbulent boundary layers at low Reynolds numbers," J. Fluid Mech., **122**, 13 (1982).

[6]G. L. Brown and A.S.W. Thomas, "Large structure in a turbulent boundary layer," Phys. Fluids, **20**, S243 (1977).

[7]B. J. Cantwell, "Organized motion in turbulent flow," Annu. Rev. Fluid Mech., **13** (1981).

[8]S. K. Robinson, "Coherent motions in the turbulent boundary layer," Annu. Rev. Fluid Mech., **23**, 601 (1991).

[9]R. F. Blackwelder and L. S. G. Kovasznay, "Time scales and correlations in a turbulent boundary layer," Phys. Fluids, **15**, 1545 (1972).

[10]R. E. Falco, "Coherent motions in the outer region of a turbulent boundary layers," Phys. Fluids, **20**, S124 (1977).

[11]C. D. Meinhart and R. J. Adrian, "On the existence of uniform momentum zones in a turbulent boundary layer," Phys. Fluids, **7**, 694 (1995).

[12]J. Zhou, R. J. Adrian, and S. Balachandar, "Auto-generation of near wall vortical structure in channel flow," Phys. Fluids, **8**, 288 (1996).

[13]J. Zhou, C. D. Meinhart, S. Balachandar, and R. J. Adrian, "Formation of hairpin packets in wall turbulence", in *Self-Sustaining Mechanisms in Wall Turbulence*, R. Panton, ed.109-134, (1997) Computational Mechanics Publications, Southampton, UK.

[14]J. Zhou, R. J. Adrian, S. Balachandar and T. Kendall, "Hairpin vortices in near-wall turbulence and their regeneration mechanisms, to appear in J. Fluid Mech. (1998).

[15]C. D. Tomkins, "A Particle Image Velocimetry Study of Coherent Structures in a Turbulent Boundary Layer", M.S. thesis, University of Illinois, Urbana, Illinois (1997).

[16]A. E. Perry, and I. Marusic, "A wall-wake model for the turbulence structure of boundary layers, Part 1. Extension of the attached eddy hypothesis," J. Fluid Mech., **298**, 361 (1995).

[17]A. E. Perry, and M. S. Chong "On the mechanism of wall turbulence," J. Fluid Mech., **119**, 173 (1982).

[18]A. E. Perry, S. Henbest, and M. S. Chong, "A theoretical and experimental study of wall turbulence," J. Fluid Mech., **165**, 163 (1986).

[19]Y. Hassan, "Experimental and Modeling Studies of Two-Point Stochastic Structure in Turbulent Pipe Flow", Ph.D. Dissertation, Univ. Illinois, Urbana, Illinois (1980).

[20]I. O. Lekakis, "Coherent Structures in Fully Developed Turbulent Pipe Flow," Ph.D. dissertation, University of Illinois, Urbana, Illinois (1988).

[21]A. E. Perry and C. J. Abell, "Scaling laws for pipe-flow turbulence," J. Fluid Mech., **67**, 257 (1975).

[22]K. J. Bullock, R. E. Cooper and F. H. Abernathy, "Structural similarity in radial correlations and spectra of longitudinal velocity fluctuations in pipe flow," J. Fluid Mech. **88**, 585 (1978).

[23]J. Komminaho, A. Lundbladh, and A. V. Johansson, "Very large structures in plane turbulent Couette flow," J. Fluid Mech. **320**, 259 (1996).

Table 1. Experimental Conditions

$Re= U_c 2R/\nu$	33,800	66,400	115,400
U_c (m/s)	4.12	8.10	14.08
u_τ (m/s)	0.201	0.373	0.60
Low-pass filter (kHz)	2.0	5.0	10.0
Sampling rate (kHz)	4.0	10.0	20.0
$y^*=\nu/ u_\tau$ (mm)	0.06	0.032	0.02
$R^+=R/ y^*$	1058	1984	3175

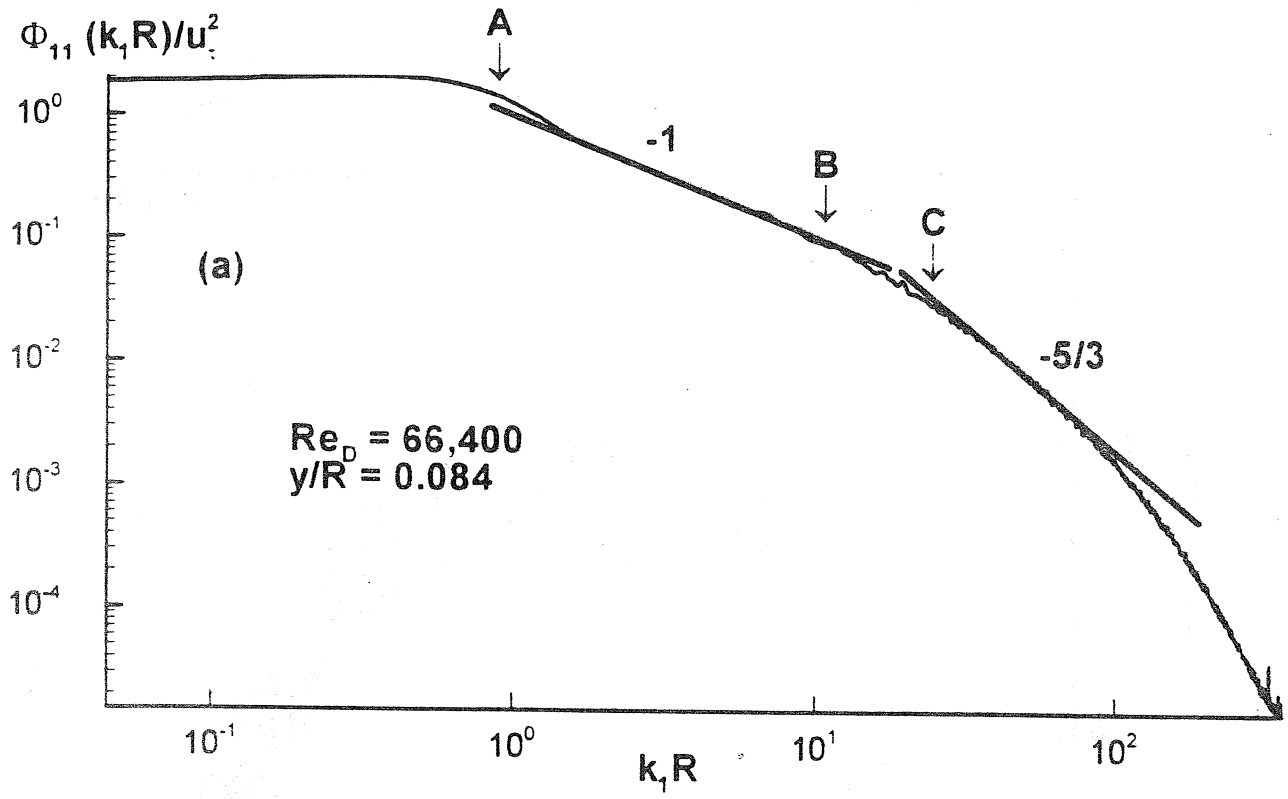

Figure 1(a) Typical power spectrum of the streamwise velocity at y/R=0.084 (y^+ = 132) plotted in conventional log-log coordinates. Re_D= 66,400. For reference 'C' denotes the start of the inertial subrange.

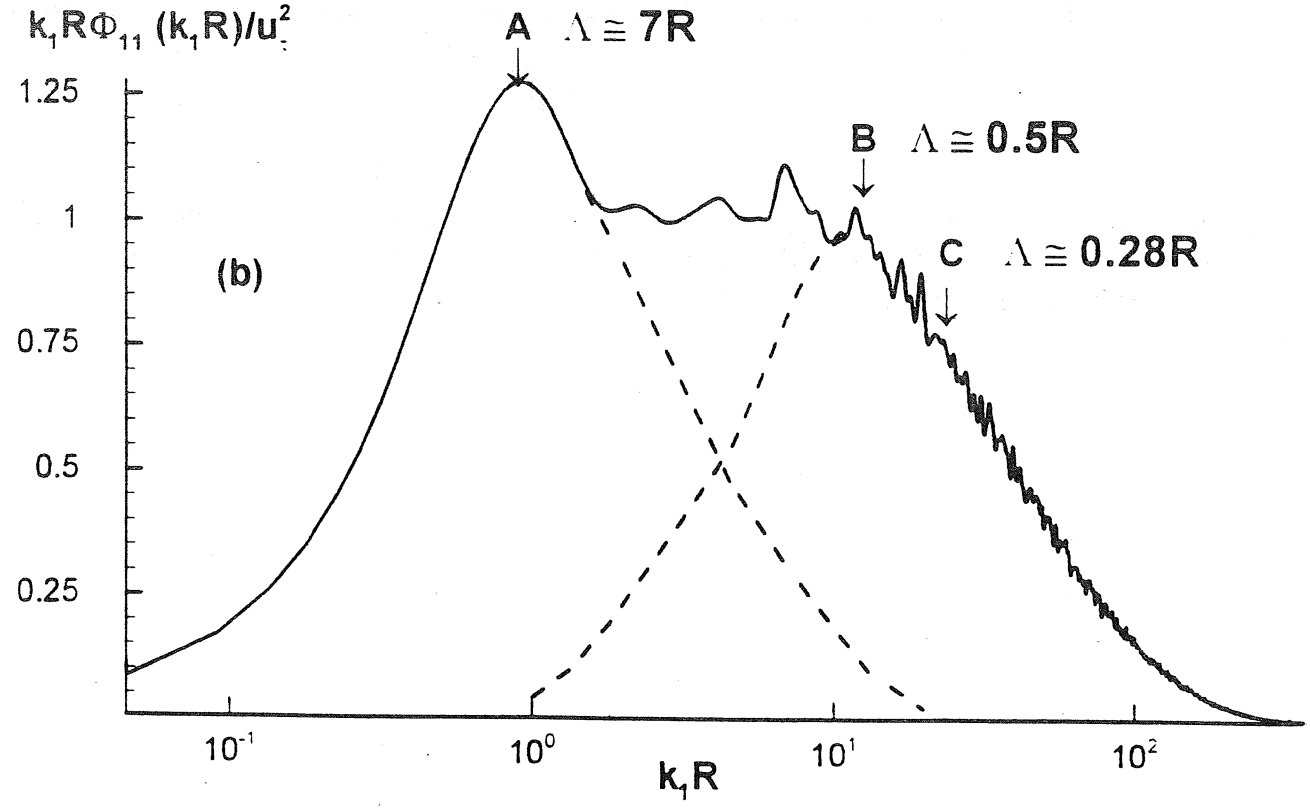

Figure 1(b). Pre-multiplied power spectrum using the same data as in (a). Dashed lines indicate the approximate shapes of the high wavenumber and low wavenumber modes, and 'A' and 'B' denote the locations of their respective maxima.

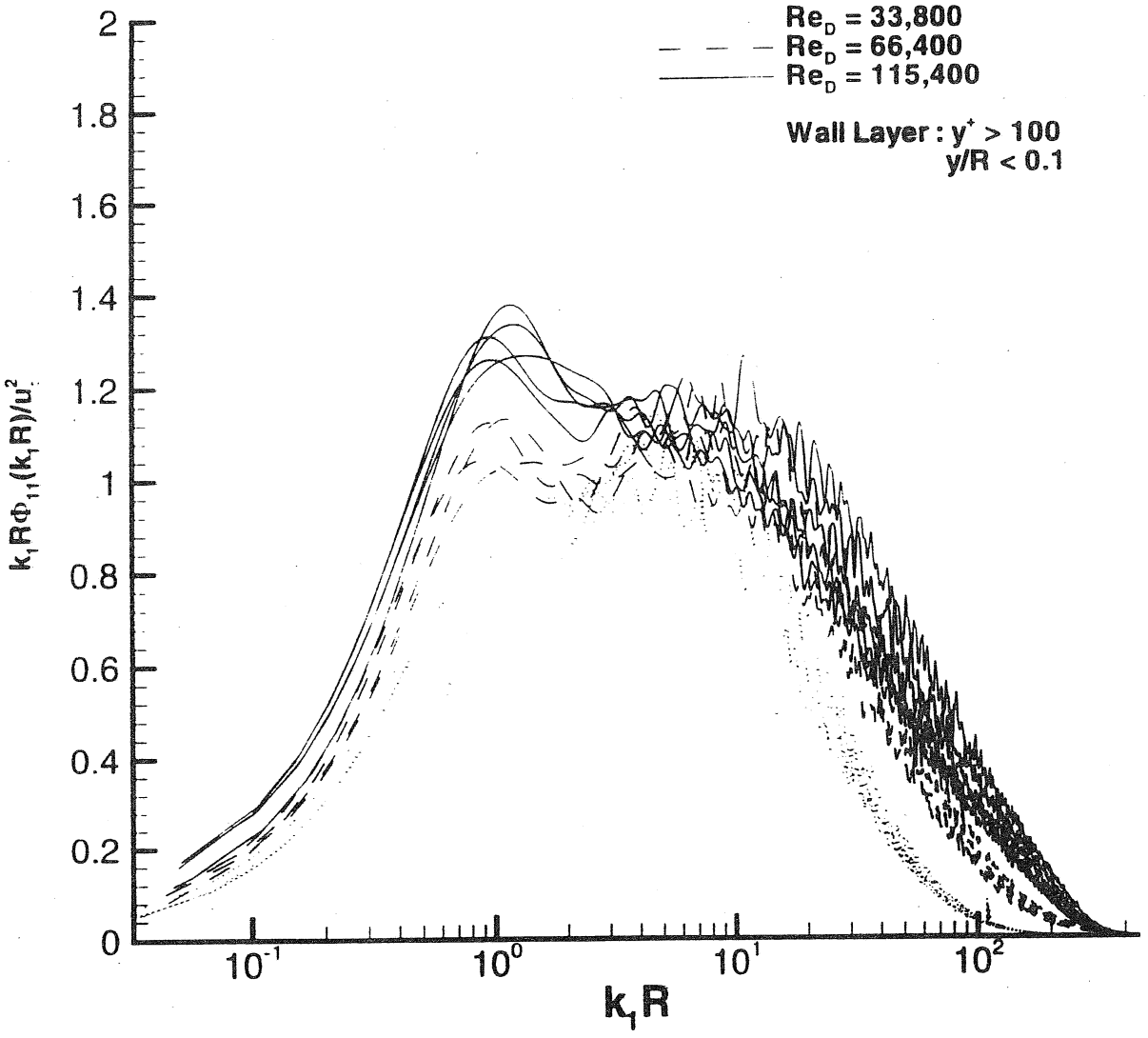

Figure 2. Pre-multiplied spectra made dimensionless using inner variables correlate at high wavenumbers over a 3.4:1 range of Reynolds numbers. The low wavenumber parts of the spectra do not correlate under this scaling.

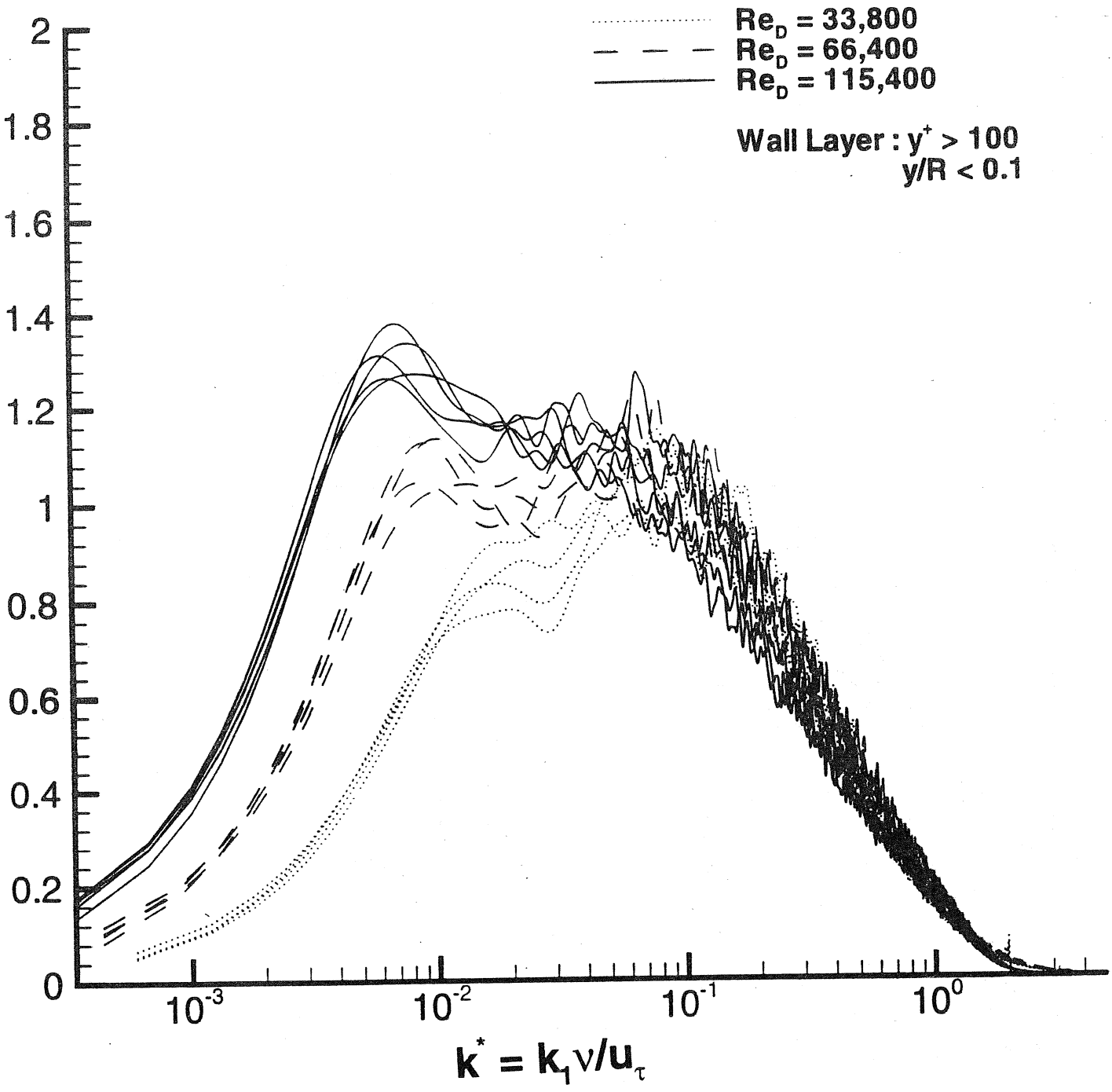

Figure 3. Pre-multiplied spectra made dimensionless using outer variables correlate at low wavenumbers over a 3.4:1 range of Reynolds numbers. The high wavenumber parts of the spectra do not correlate under this scaling.

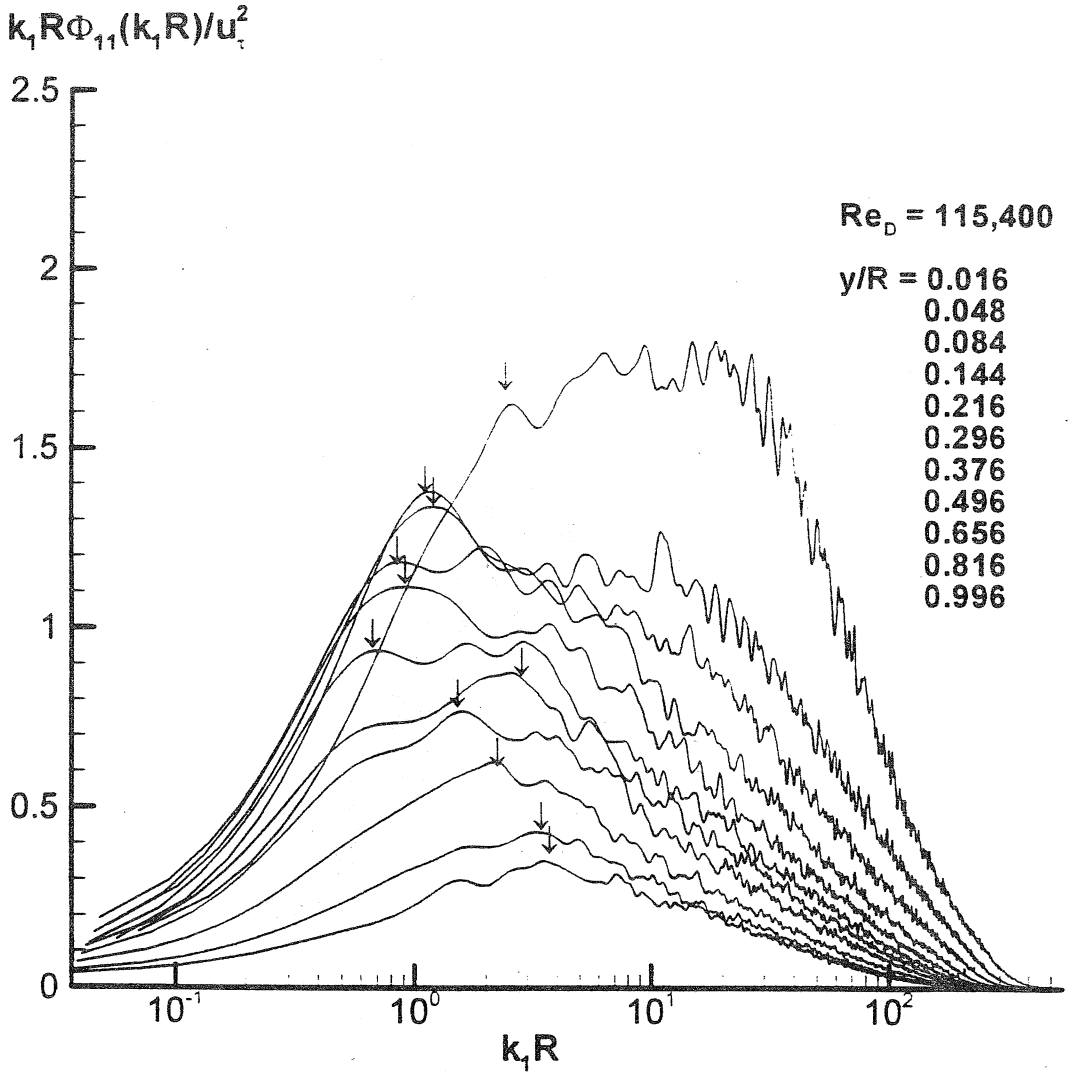

Figure 4. Pre-multiplied spectra as functions of distance from the wall. Each small arrow indicates the wavenumber of the very large-scale motion, $2\pi/\Lambda_{max}$.

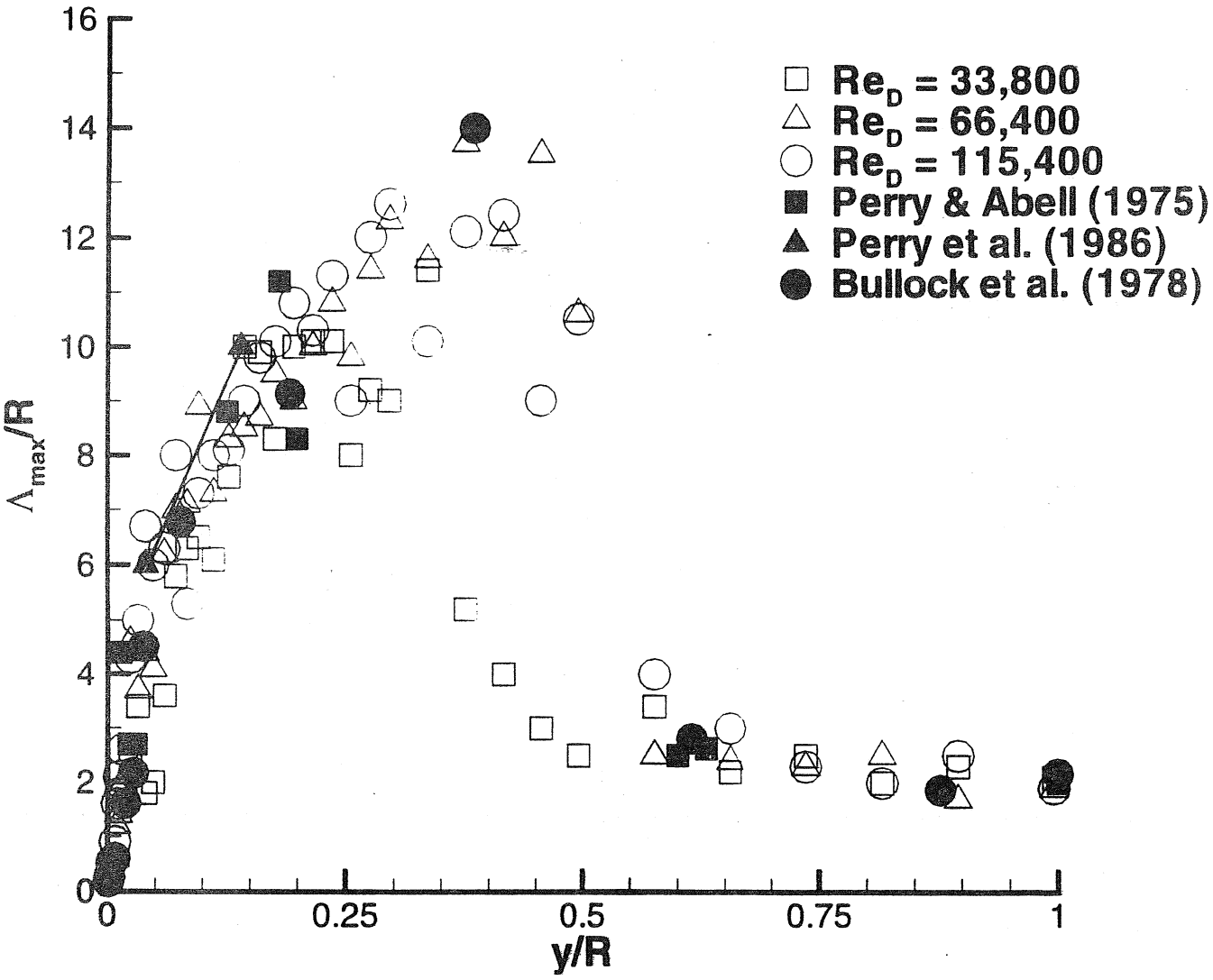

Figure 5. The dimensionless wavelength of the very large-scale motion correlates with other experiments in pipe flow (Perry and Abell[21], Bullock, *et al.*[22]) and boundary layer flow (Perry, *et al.*[18]). The maximum wavelength exceeds 14 pipe radii, and it occurs above the top of the logarithmic layer and below 0.5R.

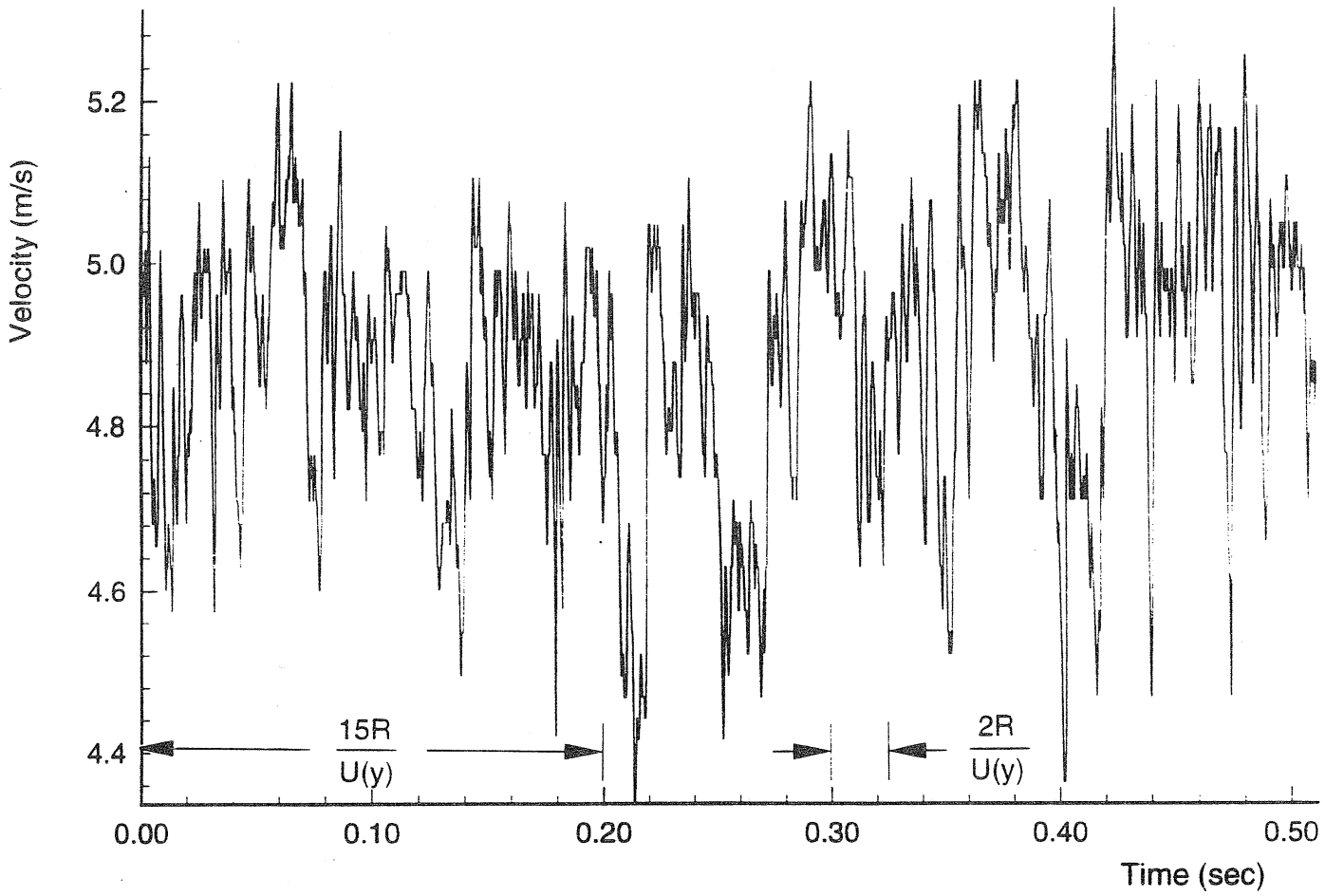

Figure 6. Time history of the streamwise velocity on the centerline. U=4.86 ms^{-1}.

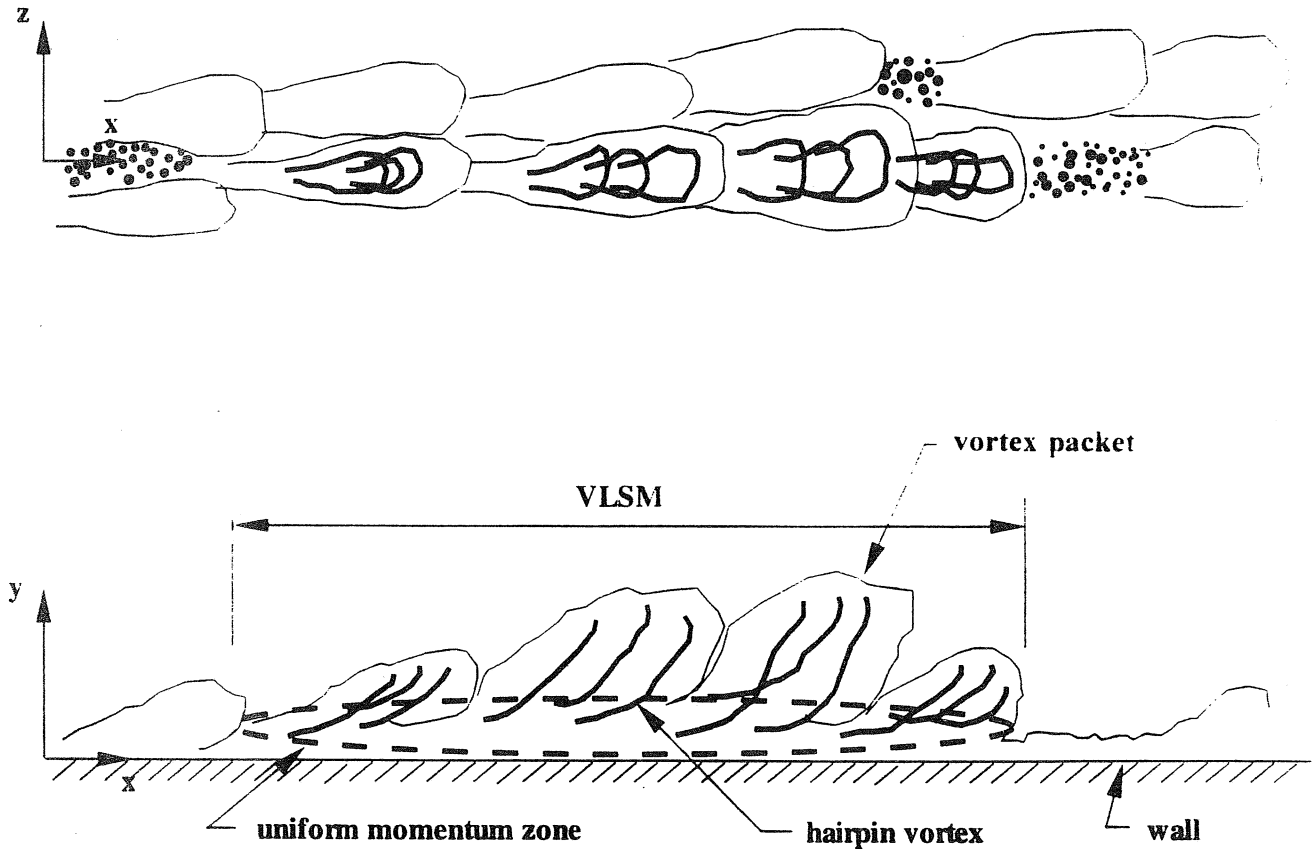

Figure 7. Conceptual model of the process that creates very large scale motions. Hairpins align coherently in groups to form long packets. and packets align coherently to form very large-scale motions

List of Recent TAM Reports

No.	Authors	Title	Date
800	Adrian, R. J.	Stochastic estimation of the structure of turbulent fields—In *Eddy Structure Identification*, J. P. Bonnet, ed. Berlin: Springer, 145–196 (1996)	Aug. 1995
801	Riahi, D. N.	Perturbation analysis and modeling for stratified turbulence	Aug. 1995
802	Thoroddsen, S. T.	Conditional sampling of dissipation in high Reynolds number turbulence—*Physics of Fluids* **8**, 1333–1335 (1996)	Aug. 1995
803	Riahi, D. N.	On the structure of an unsteady convecting mushy layer—*Acta Mechanica*, **127**, 83-96 (1998)	Aug. 1995
804	Meleshko, V. V.	Equilibrium of an elastic rectangle: The Mathieu–Inglis–Pickett solution revisited—*Journal of Elasticity* **40**, 207–238 (1995)	Aug. 1995
805	Jonnalagadda, K., G. E. Kline, and N. R. Sottos	Local displacements and load transfer in shape memory alloy composites—*Experimental Mechanics* **37**, 82–90 (1997)	Aug. 1995
806	Nimmagadda, P. B. R., and P. Sofronis	On the calculation of the matrix–reinforcement interface diffusion coefficient in composite materials at high temperatures—*Acta Metallurgica et Materialia* **44**, 2711–2716 (1996)	Aug. 1995
807	Carlson, D. E., and D. A. Tortorelli	On hyperelasticity with internal constraints—*Journal of Elasticity* **42**, 91–98 (1966)	Aug. 1995
808	Sayre, T. L., and D. N. Riahi	Oscillatory instabilities of the liquid and mushy layers during solidification of alloys under rotational constraint—*Acta Mechanica* **121** , 143–152 (1997)	Sept. 1995
809	Xin, Y.-B., and K. J. Hsia	Simulation of the brittle–ductile transition in silicon single crystals using dislocation mechanics—*Acta Metallurgica et Materialia* **45**, 1747–1759 (1997)	Oct. 1995
810	Ulysse, P., and R. E. Johnson	A plane-strain upper-bound analysis of unsymmetrical single-hole and multi-hole extrusion processes	Oct. 1995
811	Fried, E.	Continua described by a microstructural field—*Zeitschrift für angewandte Mathematik und Physik* **47**, 168–175 (1996)	Nov. 1995
812	Mittal, R., and S. Balachandar	Autogeneration of three-dimensional vortical structures in the near wake of a circular cylinder	Nov. 1995
813	Segev, R., E. Fried, and G. de Botton	Force theory for multiphase bodies—*Journal of Geometry and Physics* **20**, 371–392 (1996)	Dec. 1995
814	Weaver, R. L.	The effect of an undamped finite-degree-of-freedom "fuzzy" substructure: Numerical solutions and theoretical discussion—*Journal of the Acoustical Society of America* **100**, 3159–3164 (1996)	Jan. 1996
815	Haber, R. B., C. S. Jog, and M. P. Bendsøe	A new approach to variable-topology shape design using a constraint on perimeter—*Structural Optimization* **11**, 1–12 (1996)	Feb. 1996
816	Xu, Z.-Q., and K. J. Hsia	A numerical solution of a surface crack under cyclic hydraulic pressure loading—*ASME Journal of Tribology* **119**, 637–645 (1997)	Mar. 1996
817	Adrian, R. J.	Bibliography of particle velocimetry using imaging methods: 1917–1995—*Produced and distributed in cooperation with TSI, Inc., St. Paul, Minn.*	Mar. 1996
818	Fried, E., and G. Grach	An order-parameter based theory as a regularization of a sharp-interface theory for solid–solid phase transitions—*Archive for Rational Mechanics and Analysis* **138**, 355–404 (1997)	Mar. 1996
819	Vonderwell, M. P., and D. N. Riahi	Resonant instability mode triads in the compressible boundary-layer flow over a swept wing—*International Journal of Engineering Science* **36**, 599–624 (1998)	Mar. 1996
820	Short, M., and D. S. Stewart	Low-frequency two-dimensional linear instability of plane detonation—*Journal of Fluid Mechanics* **340**, 249–295 (1997)	Mar. 1996
821	Casagranda, A., and P. Sofronis	On the scaling laws for the consolidation of nanocrystalline powder compacts—Proceedings of the *IUTAM Symposium on the Mechanics of Granular and Porous Materials*, N. A. Fleck and A. C. F. Cocks, eds. The Netherlands: Kluwer Academic Publishers, 105–116 (1997)	Apr. 1996

List of Recent TAM Reports (cont'd)

No.	Authors	Title	Date
822	Xu, S., and D. S. Stewart	Deflagration-to-detonation transition in porous energetic materials: A comparative model study—*Journal of Engineering Mathematics* **31**, 143–172 (1997)	Apr. 1996
823	Weaver, R. L.	Mean and mean-square responses of a prototypical master/fuzzy structure—*Journal of the Acoustical Society of America* **101**, 1441–1449 (1997)	Apr. 1996
824	Fried, E.	Correspondence between a phase-field theory and a sharp-interface theory for crystal growth—*Continuum Mechanics and Thermodynamics* **9**, 33–60 (1997)	Apr. 1996
825	Students in TAM 293–294	Thirty-third student symposium on engineering mechanics, J. W. Phillips, coordinator: Selected senior projects by W. J. Fortino II, A. A. Mordock, and M. R. Sawicki	May 1995
826	Riahi, D. N.	Effects of roughness on nonlinear stationary vortices in rotating disk flows—*Mathematical and Computer Modeling* **25**, 71–82 (1997)	June 1996
827	Riahi, D. N.	Nonlinear instabilities of shear flows over rough walls, *Far East Journal of Applied Mathematics*, in press (1998)	June 1996
828	Weaver, R. L.	Multiple scattering theory for a plate with sprung masses, mean responses—*Journal of the Acoustical Society of America* **101**, 3466–3414 (1997)	July 1996
829	Moser, R. D., M. M. Rogers, and D. W. Ewing	Self-similarity of time-evolving plane wakes *Journal of Fluid Mechanics*, in press (1998)	July 1996
830	Lufrano, J. M., and P. Sofronis	Enhanced hydrogen concentrations ahead of rounded notches and cracks: Competition between plastic strain and hydrostatic stress—*Acta Metallurgica et Materialia*, in press (1998)	July 1996
831	Riahi, D. N.	Effects of surface corrugation on primary instability modes in wall-bounded shear flows	Aug. 1996
832	Bechel, V. T., and N. R. Sottos	Application of debond length measurements to examine the mechanics of fiber pushout	Aug. 1996
833	Riahi, D. N.	Effect of centrifugal and Coriolis forces on chimney convection during alloy solidification—*Journal of Crystal Growth* **179** , 287–296 (1997)	Sept. 1996
834	Cermelli, P., and E. Fried	The influence of inertia on configurational forces in a deformable solid—*Proceedings of the Royal Society of London A* **453**, 1915–1927 (1997)	Oct. 1996
835	Riahi, D. N.	On the stability of shear flows with combined temporal and spatial imperfections	Oct. 1996
836	Carranza, F. L., B. Fang, and R. B. Haber	An adaptive space–time finite element model for oxidation-driven fracture, *Computer Methods in Applied Mechanics and Engineering*, in press (1997)	Nov. 1996
837	Carranza, F. L., B. Fang, and R. B. Haber	A moving cohesive interface model for fracture in creeping materials, *Computational Mechanics* **19**, 517–521 (1997)	Nov. 1996
838	Balachandar, S., R. Mittal, and F. M. Najjar	Properties of the mean wake recirculation region in two-dimensional bluff body wakes—*Journal of Fluid Mechanics*, in press (1997)	Dec. 1996
839	Ti, B. W., W. D. O'Brien, Jr., and J. G. Harris	Measurements of coupled Rayleigh wave propagation in an elastic plate—*Journal of the Acoustical Society of America* **102**, 1528–1531	Dec. 1996
840	Phillips, W. R. C.	On finite-amplitude rotational waves in viscous shear flows—*Studies in Applied Mathematics* **100**, in press (1998)	Jan. 1997
841	Riahi, D. N.	Direct resonance analysis and modeling for a turbulent boundary layer over a corrugated surface—*Acta Mechanica*, in press (1998)	Jan. 1997
842	Liu, Z.-C., R. J. Adrian, C. D. Meinhart, and W. Lai	Structure of a turbulent boundary layer using a stereoscopic, large format video-PIV—*Developments in Laser Techniques and Fluid Mechanics*, 259–273 (1997)	Jan. 1997

List of Recent TAM Reports (cont'd)

No.	Authors	Title	Date
843	Fang, B., F. L. Carranza, and R. B. Haber	An adaptive discontinuous Galerkin method for viscoplastic analysis—*Computer Methods in Applied Mechanics and Engineering* **150**, 191–198 (1997)	Jan. 1997
844	Xu, S., T. D. Aslam, and D. S. Stewart	High-resolution numerical simulation of ideal and non-ideal compressible reacting flows with embedded internal boundaries—*Combustion Theory and Modeling* **1**, 113–142 (1997)	Jan. 1997
845	Zhou, J., C. D. Meinhart, S. Balachandar, and R. J. Adrian	Formation of coherent hairpin packets in wall turbulence—In *Self-Sustaining Mechanisms in Wall Turbulence*, R. L. Panton, ed. Southampton, UK: Computational Mechanics Publications, 109–134 (1997)	Feb. 1997
846	Lufrano, J. M., P. Sofronis, and H. K. Birnbaum	Elastoplastically accommodated hydride formation and embrittlement—*Journal of Mechanics and Physics of Solids*, in press (1998)	Feb. 1997
847	Keane, R. D., N. Fujisawa, and R. J. Adrian	Unsteady non-penetrative thermal convection from non-uniform surfaces—In *Geophysical and Astrophysical Convection*, R. Kerr, ed. (1997)	Feb. 1997
848	Aref, H., and M. Brøns	On stagnation points and streamline topology in vortex flows—*Journal of Fluid Mechanics* **370**, 1–27 (1988)	Mar. 1997
849	Asghar, S., T. Hayat, and J. G. Harris	Diffraction by a slit in an infinite porous barrier—*Wave Motion*, in press (1998)	Mar. 1997
850	Shawki, T. G., H. Aref, and J. W. Phillips	Mechanics on the Web—Proceedings of the International Conference on Engineering Education (Aug. 1997, Chicago)	Apr. 1997
851	Stewart, D. S., and J. Yao	The normal detonation shock velocity–curvature relationship for materials with non-ideal equation of state and multiple turning points—*Combustion and Flame*, in press (1998)	Apr. 1997
852	Fried, E., A. Q. Shen, and S. T. Thoroddsen	Wave patterns in a thin layer of sand within a rotating horizontal cylinder—*Physics of Fluids* **10**, 10–12 (1998)	Apr. 1997
853	Boyland, P. L., H. Aref, and M. A. Stremler	Topological fluid mechanics of stirring	Apr. 1997
854	Parker, S. J., and S. Balachandar	Viscous and inviscid instabilities of flow along a streamwise corner—*Theoretical and Computational Fluid Dynamics*, in press (1997)	May 1997
855	Soloff, S. M., R. J. Adrian, and Z.-C. Liu	Distortion compensation for generalized stereoscopic particle image velocimetry—*Measurement Science and Technology* **8**, 1–14 (1997)	May 1997
856	Zhou, Z., R. J. Adrian, S. Balachandar, and T. M. Kendall	Mechanisms for generating coherent packets of hairpin vortices in near-wall turbulence—*Journal of Fluid Mechanics*, in press (1997)	June 1997
857	Neishtadt, A. I., D. L. Vainshtein, and A. A. Vasiliev	Chaotic advection in a cubic stokes flow—*Physica D* **111**, 227 (1997).	June 1997
858	Weaver, R. L.	Ultrasonics in an aluminum foam—*Ultrasonics*, in press (1997)	July 1997
859	Riahi, D. N.	High gravity convection in a mushy layer during alloy solidification—In *Nonlinear Instability, Chaos and Turbulence*, D. N. Riahi and L. Debnath, eds., in press (1998)	July 1997
860	Najjar, F. M., and S. Balachandar	Low-frequency unsteadiness in the wake of a normal plate, *Journal of Fluid Mechanics*, in press (1997)	Aug. 1997
861	Short, M.	A parabolic linear evolution equation for cellular detonation instability	Aug. 1997
862	Short, M., and D. S. Stewart	Cellular detonation stability—I: A normal-mode linear analysis	Sept. 1997
863	Carranza, F. L., and R. B. Haber	A numerical study of intergranular fracture and oxygen embrittlement in an elastic–viscoplastic solid—*Journal of the Mechanics and Physics of Solids*, in press (1997)	Oct. 1997
864	Sakakibara, J., and R. J. Adrian	Whole-field measurement of temperature in water using two-color laser-induced fluorescence	Oct. 1997

List of Recent TAM Reports (cont'd)

No.	*Authors*	*Title*	*Date*
865	Riahi, D. N.	Effect of surface corrugation on convection in a three-dimensional finite box of fluid-saturated porous material	Oct. 1997
866	Baker, C. F., and D. N. Riahi	Three-dimensional flow instabilities during alloy solidification	Oct. 1997
867	Fried, E.	Introduction (only) to *The Physical and Mathematical Foundations of the Continuum Theory of Evolving Phase Interfaces* (book containing 14 seminal papers dedicated to Morton E. Gurtin), Berlin: Springer-Verlag, in press (1998)	Oct. 1997
868	Folguera, A., and J. G. Harris	Coupled Rayleigh surface waves in a slowly varying elastic waveguide	Oct. 1997
869	Stewart, D. S.	Detonation shock dynamics: Application for precision cutting of metal with detonation waves	Oct. 1997
870	Shrotriya, P., and N. R. Sottos	Creep and relaxation behavior of woven glass/epoxy substrates for multilayer circuit board applications	Nov. 1997
871	Riahi, D. N.	Boundary wave–vortex interaction in channel flow at high Reynolds numbers, *Fluid Dynamics Research*, in press (1998)	Nov. 1997
872	George, W. K., L. Castillo, and M. Wosnik	A theory for turbulent pipe and channel flows—paper presented at *Disquisitiones Mechanicae* (Urbana, Ill., October 1996)	Nov. 1997
873	Aslam, T. D., and D. S. Stewart	Detonation shock dynamics and comparisons with direct numerical simulation	Dec. 1997
874	Short, M., and A. K. Kapila	Blow-up in semilinear parabolic equations with weak diffusion	Dec. 1997
875	Riahi, D. N.	Analysis and modeling for a turbulent convective plume—*Applied Mathematics Letters*, in press (1998)	Jan. 1998
876	Stremler, M. A., and H. Aref	Motion of three point vortices in a periodic parallelogram	Feb. 1998
877	Dey, N., K. J. Hsia, and D. F. Socie	On the stress dependence of high-temperature static fatigue life of ceramics	Feb. 1998
878	Brown, E. N., and N. R. Sottos	Thermoelastic properties of plain weave composites for multilayer circuit board applications	Feb. 1998
879	Riahi, D. N.	On the effect of a corrugated boundary on convective motion	Feb. 1998
880	Riahi, D. N.	On a turbulent boundary layer flow over a moving wavy wall	Mar. 1998
881	Riahi, D. N.	Vortex formation and stability analysis for shear flows over combined spatially and temporally structured walls	June 1998
882	Short, M., and D. S. Stewart	The multi-dimensional stability of weak heat release detonations	June 1998
883	Fried, E., and M. E. Gurtin	Coherent solid-state phase transitions with atomic diffusion: A thermomechanical treatment—*Journal of Statistical Physics* (1998)	June 1998
884	Langford, J. A., and R. D. Moser	Optimal large-eddy simulation formulations for isotropic turbulence	July 1998
885	Riahi, D. N.	Boundary-layer theory of magnetohydrodynamic turbulent convection	Aug. 1998
886	Riahi, D. N.	Nonlinear thermal instability in spherical shells	Aug. 1998
887	Riahi, D. N.	Effects of rotation on fully non-axisymmetric chimney convection during alloy solidification	Sept. 1998
888	Fried, E., and S. Sellers	The Debye theory of rotary diffusion	Sept. 1998
889	Short, M., A. K. Kapila, and J. J. Quirk	The hydrodynamic mechanisms of pulsating detonation wave instability	Sept. 1998
890	Stewart, D. S.	The shock dynamics of multidimensional condensed and gas phase detonations	Sept. 1998
891	Kim, K. C., and R. J. Adrian	Very large-scale motion in the outer layer	Oct. 1998